
CHICAGO JOURNALS

Tectonic Implications and Morphology of Trapezoidal Mica Grains from the Sutlej Section of the Higher Himalayan Shear Zone, Indian Himalaya
Author(s): Soumyajit Mukherjee
Reviewed work(s):
Source: *The Journal of Geology*, Vol. 120, No. 5 (September 2012), pp. 575-590
Published by: The University of Chicago Press
Stable URL: http://www.jstor.org/stable/10.1086/666744
Accessed: 20/08/2012 10:11

Your use of the JSTOR archive indicates your acceptance of the Terms & Conditions of Use, available at
http://www.jstor.org/page/info/about/policies/terms.jsp

JSTOR is a not-for-profit service that helps scholars, researchers, and students discover, use, and build upon a wide range of content in a trusted digital archive. We use information technology and tools to increase productivity and facilitate new forms of scholarship. For more information about JSTOR, please contact support@jstor.org.


The University of Chicago Press is collaborating with JSTOR to digitize, preserve and extend access to *The Journal of Geology.*

http://www.jstor.org

Tectonic Implications and Morphology of Trapezoidal Mica Grains from the Sutlej Section of the Higher Himalayan Shear Zone, Indian Himalaya

*Soumyajit Mukherjee**

Department of Earth Sciences, Indian Institute of Technology Bombay, Powai, Mumbai 400 076, Maharashtra, India

ABSTRACT

Microscopic trapezoidal micas are reported from the Sutlej section of the Higher Himalayan Shear Zone, India, and are attributed to an up-dip top-to-southwest sense of brittle shear along *C* planes of preexisting ductile shear dipping northeast. The longest margins of these trapezoids dip northeast and are oblique to either the *C* planes or their enveloping planes. Intragrain slips along cleavages aided their thrusting, while the surrounding competent quartzofeldspathic minerals resisted it. The cleavages of the trapezoids are parallel to their longest margins. These cleavages, the longest margins, the overall asymmetry of trapezoid aggregates, and the trails emanating from their corners are reliable indicators of brittle shear sense. Trails broken from the corners of developing trapezoids define both the *P* and the *Y* shear planes. Subcircular stacks and triangular mineral grains are also possible variations of trapezoids. Some of the trapezoidal micas were products of ductile-brittle deformation. Variable intensities of dynamic recrystallization around the trapezoid margins indicate the rock did not strain-harden uniformly. The nongenetic interlinked morphological parameters of the trapezoid aspect ratio, internal angles, and local orientation vary widely and partially define the orientation and the geometry of the trapezoids. Further studies of the three-dimensional shapes and genesis of trapezoidal minerals are planned.

> Many structural geologists look at the physical or structural aspects of minerals and rocks, especially from the viewpoint of deformation processes and preferred orientations of grains, without being concerned about the chemical aspects of these processes. (Vernon 2004)

Introduction

Ductile shearing of rocks on meso- and microscopic scales may result in sigmoid-, lenticular-, and parallelogram-shaped mineral grains (Lister and Snoke 1984; ten Grotenhuis 2003; Passchier and Trouw 2005; Mukherjee 2011). Symmetric and asymmetric sigmoid- and lens-shaped duplexes are common structures attributed to mesoscale brittle shear (e.g., McClay 1992). By contrast, trapezoidal mineral grains have been merely photomicrographed in other studies (e.g., Mukherjee 2007, 2008, 2010*a*, 2010*b*; Mukherjee and Koyi 2010*a*, 2010*b*; fig. 12.40 of Trouw et al. 2010) but have not received the attention they deserve.

Manuscript received December 3, 2011; accepted April 15, 2012.

* E-mail: soumyajitm@gmail.com.

A trapezoid is a quadrilateral with only a single pair of parallel sides. A review of the literature reveals a number of examples of trapezoidal grains or aggregates (figs. 1, 2). These include (i) conjugate normal (or thrust) mesoscopic faults leading to trapezoidal grabens (or horsts) in profile views (fig. 1*ia*, 1*ib*; e.g., Twiss and Moores 2007); (ii) extensional shear-fracture boudins where trapezoids and their inverted equivalents alternate in trains (fig. 1*ii*; Mandal et al. 2000; also see fig. 14.5 of Fossen 2010); (iii) folding of rectangular boudinaged layers may result in trapezoidal clasts with notches (fig. 1*iii*; Sengupta 1983); (iv) intersecting irregular fractures (in rocks) that may generate quasi trapezoids, as are seen in basalts (fig. 1*iv*; S. Mukherjee, unpublished observation); (v) anastomosing foliations that enclose trapezoidal microlithons (fig. 1*v*; Powell 1979,

[The Journal of Geology, 2012, volume 120, p. 575–590] © 2012 by The University of Chicago. All rights reserved. 0022-1376/2012/12005-0006$15.00. DOI: 10.1086/666744

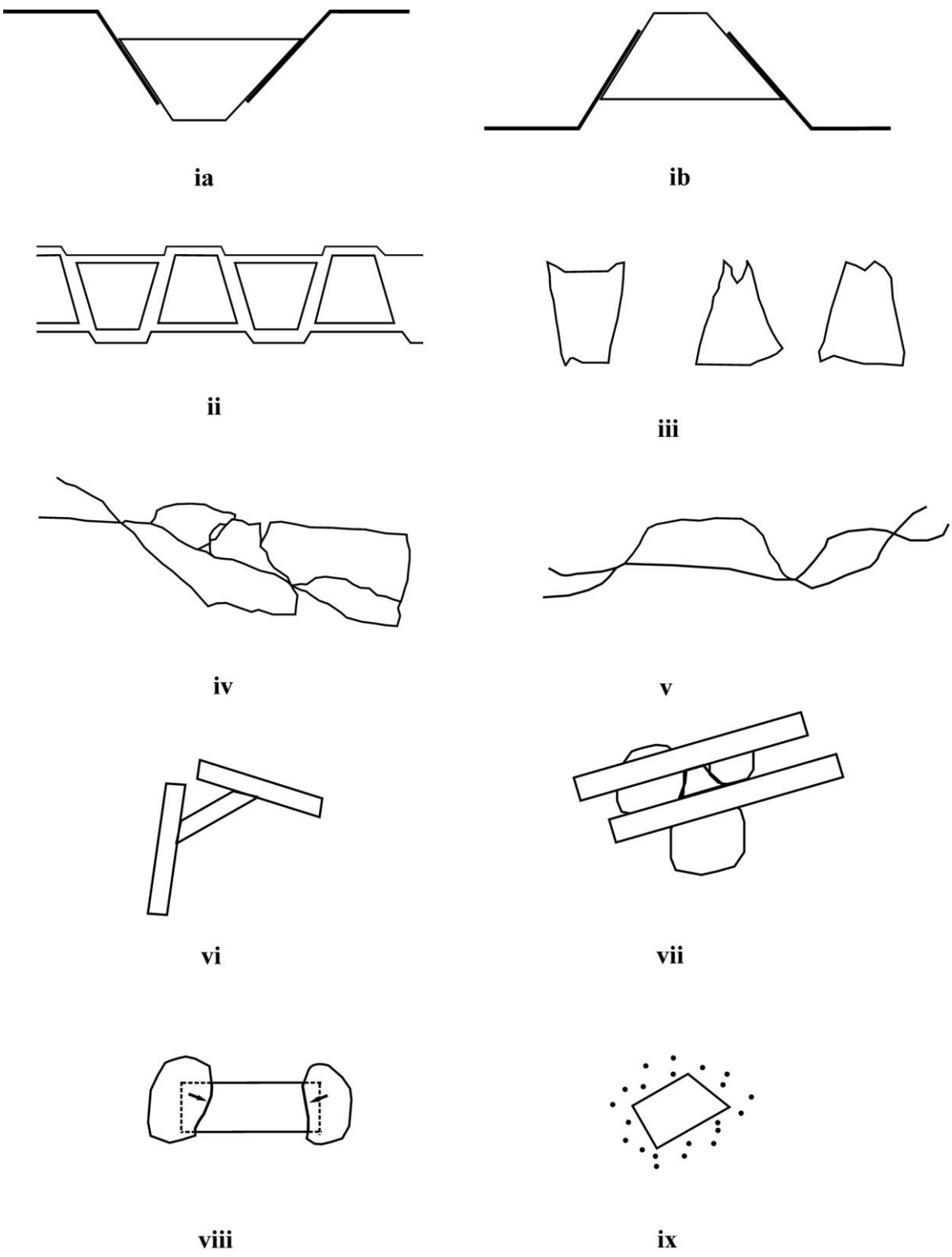

Figure 1. Trapezoid-shaped fabrics and structures. *ia*, graben structure; *ib*, horst structure; *ii*, extensional shear-fracture boudins (drawn from fig. 1*c* of Mandal et al. 2000); *iii*, boudins with notches (drawn from figs. 11*c*, 12*c* of Sengupta 1983); *iv*, irregular fractures (drawn from fig. 12 of Bahat 1987); *v*, anastomosing foliation and bounding microlithons; *vi*, *vii*, overlap of grains in different situations; *viii*, window structure; *ix*, rock fragment in a sedimentary matrix. A color version of this figure is available in the online edition or from the *Journal of Geology* office.

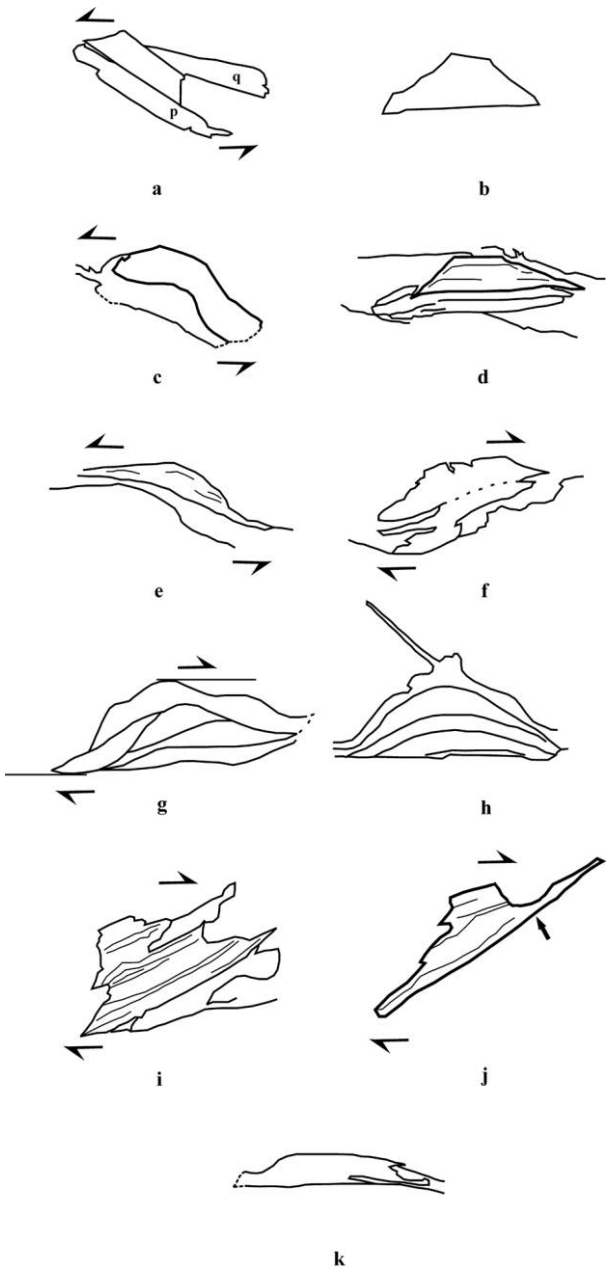

as referred to in Davis and Reynolds 1996); (vi) haphazard overlap of microscopic rectangular (mica) grains in a decussate texture (fig. 1*vi*; Vernon 2004); (vii) overlap of two rectangular grains in the intergrain space among three other anhedral grains as seen in some thin sections of sandstones (fig. 1*vii*); and (viii) migration of adjacent mica grain boundaries to generate microscopic trapezoidal "window structures" (fig. 1*viii*; Jessel 1987; e.g., fig. 11 of Mukherjee and Koyi 2010*b*). The migrated grain boundaries that defined such trapezoids are characteristically curved. In a rare instance (case ix), trapezoidal mélanges have been reported as boudins by Alonso et al. (2006) between regionally straight foliation planes (fig. 1*ix*). Since these boudins could also be exotic blocks, Alonso et al. (2006) rightfully did not speculate on their genesis. In a presumably similar case, isolated trapezoidal clasts in other sedimentary rocks have also been documented (e.g., fig. 4*a* of Hölgel et al. 2006). Such trapezoidal clasts are produced by random breakage from the parent rocks. Finally, (x) as a by-product of a tectonic study, Mukherjee and Koyi (2010*b*) reported trapezoids of high-grade and rigid staurolites (drawn as fig. 2) from thin sections of the rocks of the Zanskar Shear Zone, which is the northern boundary of the Higher Indian Himalaya. Likewise, Mukherjee and Koyi (2010*a*, drawn as fig. 2; also Mukherjee 2007, 2008) reported very briefly on the trapezoidal micas from the Indian Higher Himalaya in the Sutlej section. Repeated occurrences of trapezoid-shaped micas were a new microstructural observation and were not possible to explain inexplicably by any known deformation mechanism.

Microscopic trapezoidal minerals have been postulated as evidence of thrusting on the grain scale (fig. 2; Mukherjee 2007, 2008, 2010*a*, 2010*b*; Mukherjee and Koyi 2010*a*, 2010*b*). The key reason was that under an optical microscope, the longest margins of trapezoids were found to dip northeast, parallel to nearby brittle shear *Y* planes. (The primary shear planes are represented by *Y*, and the

Figure 2. Previously reported trapezoid-shaped grains in our published work; few adjacent grains are outlined. The dashed lines in *c*, *f*, and *g* are the possible grain boundaries. Thinner lines are the cleavage planes. Except staurolite grains in *h*, all other outlines of trapezoids are micas. In *a*, while the trapezoid thrust along the margin of another grain (p), the former cut across another grain (q). A few cases of trapezoid shapes (*c*, *e–k*) are found and few others depart from the shape in the strictest sense (*a*, *b*, *d*). Trapezoids in *a*, *c*, *e–g*, *i*, and *j* give (a top-to-southwest) shear sense. The other trapezoids in *b*, *d*, *h*, and *k* do not reveal any shear sense (since their longest margins are parallel to the *Y* planes). "Enveloping lines" of an aggregate of trapezoids are defined in *g*, and the "longest margin" (full arrow) in *j*. Grains in *a–d* are outlined from figure 12*a*–12*d* of Mukherjee and Koyi (2010*a*); *e–h* from fig. 9*a*–9*d* and *i–k* from fig. 10*b*–10*d* of Mukherjee and Koyi (2010*b*). *a–d* are from the Sutlej section of the Higher Himalayan Shear Zone, whereas the others are from the Zanskar Shear Zone. A color version of this figure is available in the online edition or from the *Journal of Geology* office.

brittle planes that are oblique to them are the *P* planes; review in Passchier and Trouw 2005, their fig. 5.50.) These authors presented the following different modes of occurrences for the trapezoid-shaped micas, namely, (i) one trapezoid grain thrust over another along the longest margin of the former; (ii) isolated biotite trapezoids that are completely surrounded by quartzofeldspathic minerals; (iii) instead of a single grain of muscovite, a number of muscovite grains define an aggregate of trapezoids; (iv) the longest margin of the trapezoid is wavy; (v) the longest margin of muscovite trapezoids are juxtaposed against other muscovite grains; (vi) muscovite trapezoids are juxtaposed with quartzofeldspathic minerals; (vii) an aggregate of muscovite grains that together define a number of thrust slices wherein only one muscovite grain is trapezoid shaped, (viii) symmetrically and asymmetrically stacked staurolite grains where the former stacks do not reveal any shear sense. Mukherjee and Koyi (2010*b*) also described trapezoid-shaped micas where the nonparallel sides are convex toward the grains themselves. Such shapes were interpreted as products of grain boundary migration and not as brittle shear.

From the Sutlej section of the Higher Himalayan Shear Zone (HHSZ) in the western Indian Himalaya, this work enumerates Mukherjee's (2007, 2010*a*, 2010*b*) and Mukherjee and Koyi's (2010*a*, 2010*b*) observations on trapezoidal mineral grains and details: (i) their morphological variations; (ii) definition and estimation of parameters related to their shapes and orientation; and (iii) their brittle shear sense. Thus, it is the first dedicated work on the trapezoid-shaped grains.

Geology of the Study Area

The HHSZ is exposed in the Sutlej River section (fig. 3) in the Kinnaur district of Himachal Pradesh (India). Here the HHSZ consists of gneisses and schists of Precambrian and Proterozoic ages. The rocks were metamorphosed at dominantly greenschist to amphibolite facies (Grasemann et al. 1999; Vannay et al. 1999; Vannay and Grasemann 2001). Two strands of the Main Central Thrust are exposed—one that skirts the underlying Lesser Himalayan Larji-Kulu-Rampur Window of sedimentary rocks and another that passes through Karcham as the MCT-upper (MCT_U). Rocks northeast of the MCT_U belong to the Vaikrita Group (Srikantia and Bhargava 1998). Mukherjee (2010*b*) presented a detailed photographic description of structures of this shear zone from field and microscopic studies. Mukherjee and Koyi (2010*a*) grouped rocks from Karcham up to Shongthong in the northeast along the river section as nonmigmatitic and Shongthong to the northern extremity of the HHSZ as migmatitic rocks. The thin sections studied in this work come from both the migmatitic and the nonmigmatitic rocks. These rocks are located northeast of the MCT_U.

The upper part of the HHSZ, from the MCT_U up to the northern boundary of the shear zone, underwent three dominant deformation and extrusion phases (Mukherjee and Koyi 2010*a*). These were (i) E_1, top-to-southwest ductile shear (also see Mukherjee 2012*a*) during ~25–19 Ma, and (ii) E_2, a combination of simple shear and channel flow during ~15–12 Ma. Top-to-northeast extensional shear developed inside the South Tibetan Detachment System–upper ($STDS_U$) and the South Tibetan Detachment System–lower ($STDS_L$); (iii) a pre–12 Ma event of top-to-southwest of brittle shear (also see Mukherjee 2012*b*). The earlier *C* planes of ductile shear latter reactivated as the *Y* planes of brittle shear. A component of pure shear has also been quantified in terms of a kinematic vorticity number of 0.86 (Grasemann et al. 1999) and 0.73–0.81 (Law et al. 2011). Based on U-Th-Pb dates of monazite, it has very recently been shown that the HHSZ in the Sutlej section extruded by channel-flow and critical-taper mechanisms in a flipping mode (Chambers et al. 2011; S. Mukherjee, unpublished manuscript).

Genesis, Shear Sense, and Morphometry

The *XZ*-oriented thin sections of rocks of the HHSZ, Sutlej, section reveal trapezoidal mica grains (figs. 4, 5*a*, 5*c*, 5*d*, 7*a*, 7*b*, 8*b*–8*d*; also see fig. 3*a*–3*c* of Holyoke and Tullis 2006 for comparison) or aggregates in stacks (figs. 7*c*, 10*b*–10*d*) that are usually of muscovite ± biotite ± chlorite. Being comparatively incompetent (weak), micas are expected to exhibit higher strains than any surrounding quartzofeldspathic minerals (Blenkinsop 2000; Passchier and Trouw 2005; Mukherjee 2011). One of the two parallel margins of individual trapezoids that are longer than the other three margins is referred throughout this work as the "longest margin" (full arrow in fig. 2*j*).

The trapezoidal mica grains reported here cannot be explained by any of hypotheses (i) to (ix) in the previous section (fig. 1). For example, (i), they cannot obviously be compared with mesoscopic grabens or horsts. This is because there is no microscopic evidence that the nonparallel margins of those trapezoids underwent brittle displacement with respect to any adjacent counterpart mineral

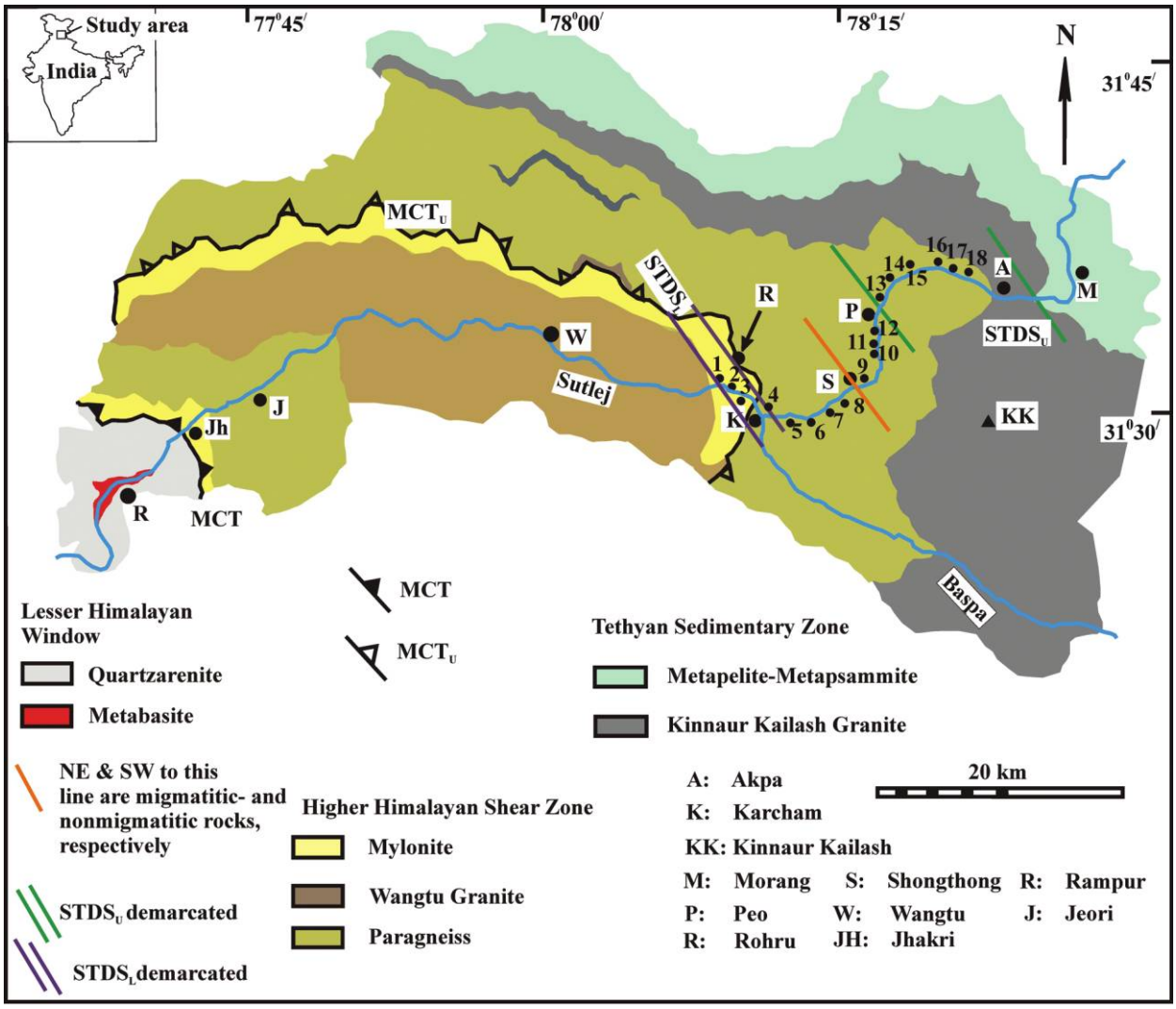

Figure 3. Geological map of the Higher Himalayan Shear Zone (from Singh 1993; Srikantia and Bhargava 1998; and Vannay and Grasemann 2001). The location of the Main Central Thrust (MCT) is as per Singh (1993). Srikantia and Bhargava's (1998) Vaikrita Thrust is denoted by Godin et al.'s (2006) "MCT-upper" (MCT_U). The lower and upper strands of extensional ductile shear zones—South Tibetan Detachment System $STDS_L$ and the $STDS_U$—are shown as per Mukherjee and Koyi (2010*a*). 1–18 = sample locations.

grains. In almost all cases, the two nonparallel margins of mica trapezoids are in contact with quartzofeldspathic minerals, that is, with other minerals. (ii) Had they been shear boudins, these trapezoids would occur in trains. Secondly, the foliation planes in the matrix minerals that bound them show no sign of being deflected into the intertrapezoid spaces. None of the observed trapezoids occur along a line, and none are wrapped by the foliation. Deflection of foliation at the intertrapezoid space would indicate that those trapezoids at one time were joined together and later pulled apart. The void created between the pulled-apart grain is occupied by materials from the matrix (e.g., Hippertt 1993; Singh 1999). (iii) The straight foliations bounding the trapezoids (Mukherjee 2007, 2008, 2010*a*, 2010*b*; Mukherjee and Koyi 2010*a*) preclude their genesis by folding of preexisting rectangular boudins. (iv) Similarly, the lack of fractures surrounding the trapezoids negates their origin by brittle failure. (v) The foliations in these thin sections are straight and do not anastomose. The studied trapezoids are larger than microlithons and sometimes the former are single grains. Trapezoids of single minerals are quite unlike microlithons; the latter usually consist of aggregates of minerals of two different sizes and habits (see fig. 11.4 of Twiss and Moores 2007). (vi) The quartzofeldspathic min-

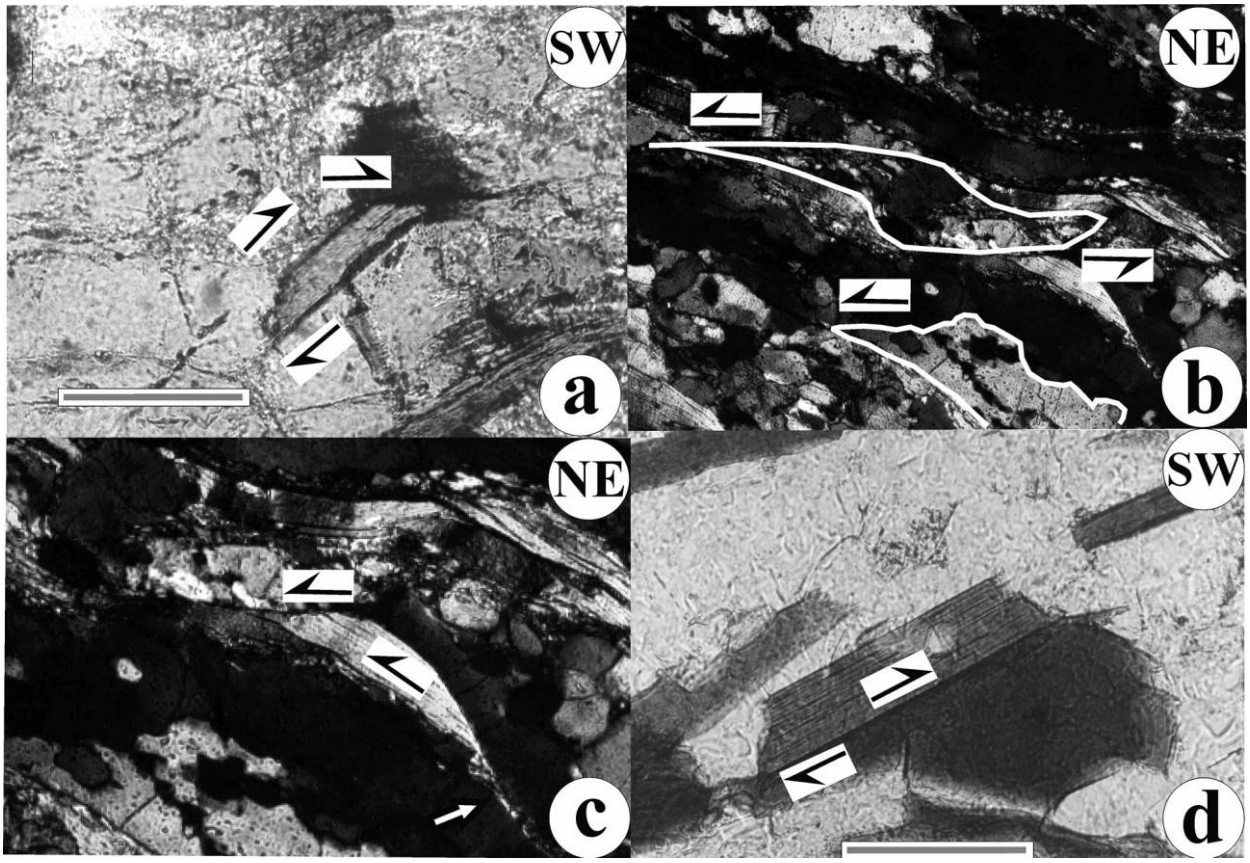

Figure 4. A top-to-southwest sense of brittle shear is displayed by mica trapezoids. In *a* and *d*, the *Y* planes are extrapolated from outside the field of view. *a*, Biotite trapezoid with straight margins unaffected by recrystallization thrust over two quartzofeldspathic minerals. Photo in plane-polarized light; photo length = 5 mm; sample 8. *b*, Two aggregates of quartzofeldspathic minerals (white borders) demonstrate a prior ductile shear sense that matches with the late brittle shear indicated by the biotite trapezoid with straight margins and no recrystallization. The trapezoid is magnified in *c*, where a recrystallized tail (arrow) also defines the *P* plane. *b* and *c* are in cross-polarized light; sample 12. Photo length in *c* is 2.5 mm. *d*, Biotite trapezoid with straight margins devoid of any recrystallization thrust over an irregular-shape biotite grain. Photo in plane-polarized light. Photo length = 5 mm; sample 17. A color version of this figure is available in the online edition or from the *Journal of Geology* office.

erals that always bound the nonparallel boundaries of trapezoids invalidate the possibility that they develop by overlap of a number of subhedral mica grains. (vii) Trapezoidal intergrain spaces formed due to overlap of subhedral mineral grains are confined to clastic sedimentary rocks (Pettijohn 1984). This situation is most unlikely in metamorphic rocks without intergranular spaces. (viii) The remarkably straight margins of some of the trapezoids imply that they are unlikely to be shaped by grain boundary migration. (ix) Since the observed trapezoidal mica grains occur in mylonites, it is implausible that they are remnant exotic or transported rock fragments.

None of the trapezoidal grains presented here (figs. 4–10) match any of the previously well-established geometries of ductile shear fabrics, namely, sigmoidal, lenticular, or parallelogram. The second reason for not attributing them to ductile shears is that their longest margins dip northeast throughout the HHSZ. This also includes the two ductile extensional shear zones—the $STDS_U$ and the $STDS_L$—where intense top-to-northeast ductile shear gave rise to southwest-dipping ductile shear fabrics. Thus, the inclination of the trapezoids (later defined as the "local orientation") is opposite to the fabrics related to the latest and most intense ductile deformation within the $STDS_U$ and the $STDS_L$. In addition, the trapezoids are not products of specific orientation of cross-sectioning of mica grains in thin sections. If mica grains could yield trapezoidal shapes in thin sections from their initial random

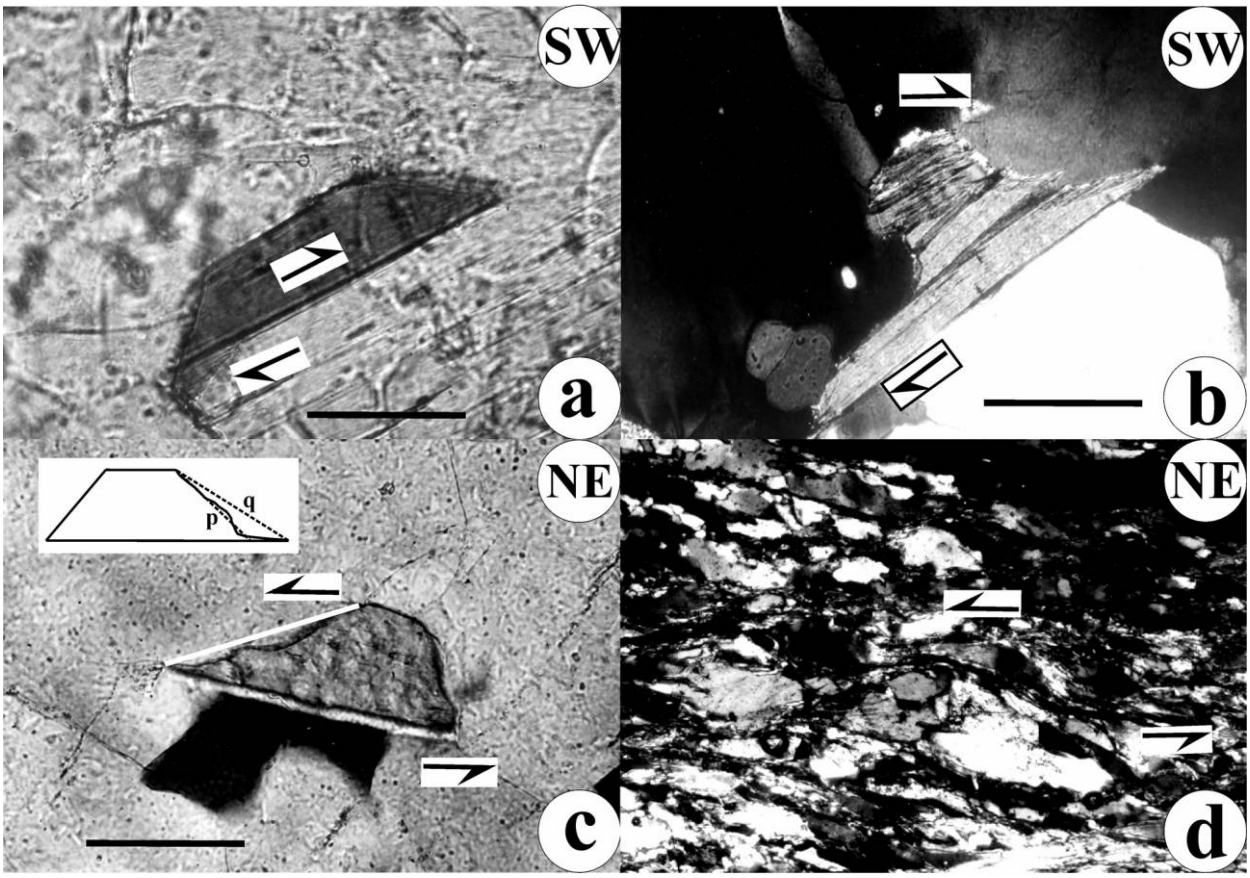

Figure 5. Top-to-southwest brittle shear indicated by northeast-dipping longest margins of micas. *a–c*, the *Y* planes (black lines) are extrapolated from outside the field of view. *a*, Trapezoid biotite possesses remarkably straight margins, escaped recrystallization, and thrust over a muscovite grain. Photo length = 1.3 mm; photo in plane-polarized light; sample 2. *b*, Stacked trapezoids of biotites. Individual grains have minor variations in geometry and orientation. The biotite grain in contact with quartz is almost straight. Photo length = 2.5 mm; photo in plane-polarized light; sample 6. *c*, Trapezoidal muscovite with curvilinear nonparallel sides. The inclined white line is the approximated margin considered for the measurement of the internal angle (especially shown in the inset). Photo length = 1.3 mm; photo in cross-polarized light; sample 14. *d*, Biotite trapezoid thrust over a larger sigmoid quartz fish. Photo length = 5 mm; photo in cross-polarized light; sample 3. A color version of this figure is available in the online edition or from the *Journal of Geology* office.

orientations, then those trapezoids are also expected to be haphazardly disposed. This is also not the case.

On the other hand, mesoscopic thrust slices or duplexes with *P* planes dipping uniformly north or northeast (oblique to the *C* plane) demonstrate a uniform top-to-southwest sense of brittle shear throughout the HHSZ in the study area (fig. 3.7*a*–3.7*d* of Mukherjee 2007; fig. 11*a*–11*d* of Mukherjee and Koyi 2010*a*; figs. 22*a*–22*c*, 23*a*–23*d*, 24 of Mukherjee 2011). Since no existing genetic theories account for the trapezoids and their longest margins always dip northeast and either are at an angle to the *C* planes (figs. 4–7) or the lines envelope the trapezoids parallel the *C* planes (figs. 8–10), these trapezoid shapes are proposed to be grain-scale products of a top-to-southwest brittle shear. This conjecture receives support from observations that the microscopic ductile shear *C* planes abruptly truncate anhedral mineral grains such as quartz (fig. 8*a*). This indicates that those planes also record a late-phase brittle deformation and when the longest margin of the trapezoid-shaped grain is in contact with another grain of the same mineral species exhibiting equal brightness at all microscopic orientations in plane- and cross-polarized lights (figs. 6*d*, 7*b*, 7*c*, 8*a*, 9*b*, 10*d*). These observations indicate that those two grains were originally a part of a

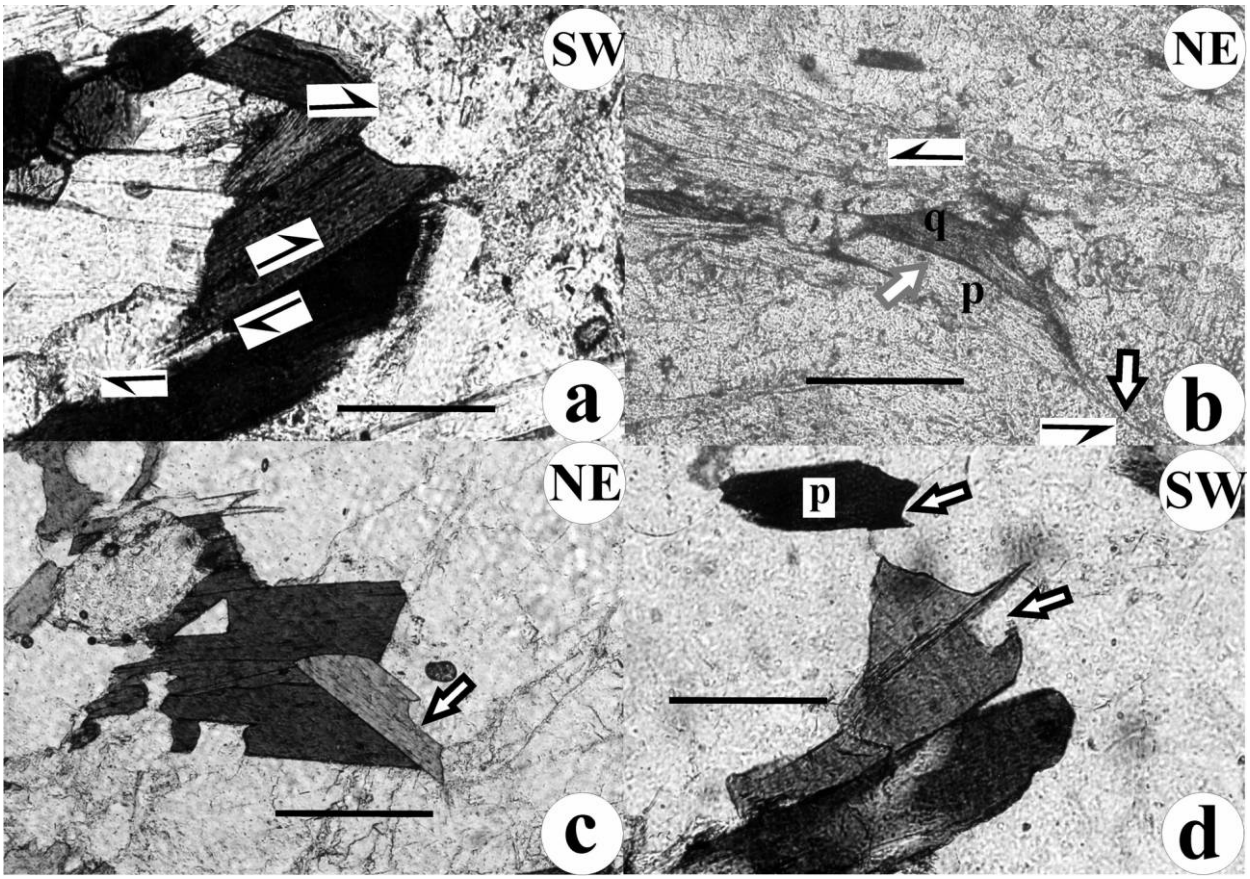

Figure 6. Thrust-over biotite grains with northeast-dipping longest margins display a top-to-southwest brittle shear. The *Y* planes (black lines) are extrapolated from outside the field of view. All photos in plane-polarized light. *a*, The longest margin is very gently curved, and so are the cleavages. Photo length = 2.5 mm; sample 1. *b*, Muscovite (grain p) and a superjacent biotite trapezoid (grain q) display the same shear sense. Both the grains are feebly kinked (arrow, center. A trail (lower arrow) from the longest margin of the muscovite grain is the prolongation of the *P* shear plane. Photo length = 2.5 mm; sample 2. *c*, Biotite trapezoid thrust over an aggregate of biotite grains in a top-to-southwest brittle shear sense. A part of its parallel margins underwent migration of adjacent quartzofeldspathic minerals (arrow). Photo length = 2.5 mm; sample 5. *d*, A biotite grain that looks triangular with the present magnification, thrust over another biotite grain and the quartzofeldspathic matrix. Grain boundary migration noticed in the underthrust grain and also elsewhere at another biotite grain p (arrows) Photo length = 2.5 mm; sample 4. A color version of this figure is available in the online edition or from the *Journal of Geology* office.

precursor single grain that later underwent relative translation without rotation consistent with brittle slip. However, there also are cases where the two grains of the same species in contact have different brightness (figs. 4*d*, 6*a*). In this work, a number of trapezoids reveal the same shear sense as other shear sense indicators in the same field of view (figs. 4*b*, 5*d*, 7*b*, 10*a*). In the other photomicrographs, no additional shear sense indicators are present (figs. 4, 5*a*–5*c*, 6, 7*a*–7*c*, 8, 9, 10*b*–10*d*). In the latter cases, where the longest margins of the trapezoids are inclined to the brittle shear *Y* planes (figs. 4, 5*a*–5*c*, 6, 7*a*–7*c*, 8*b*), the brittle shear sense is bases solely on the inclination of the longest margin of the trapezoids. The top-to-southwest brittle shear sense anticipated in all these microscopic cases match the macroscopic brittle shear sense established by field studies from the HHSZ by Mukherjee (2007, 2010*b*), Mukherjee and Koyi (2010*a*).

The longest margins of the trapezoids are considered as the *P* planes since they are inclined at an angle to the brittle shear *Y* planes. The longest margins may be straight (fig. 5*a* is the best example, but see also figs. 5*d*, 6*c*, 6*d*, 7*a*, 9*d*) at a given magnification or are curved to various extent (figs. 5*b*, 5*c*, 6*a*, 7*b*, 7*c*, 9*b*, 9*c*, 10*b*). As has been noted for ductile deformed isolated mineral fish (e.g., Mukherjee 2010*a* [fig. 8*b*], 2010*b*, 2011), those trape-

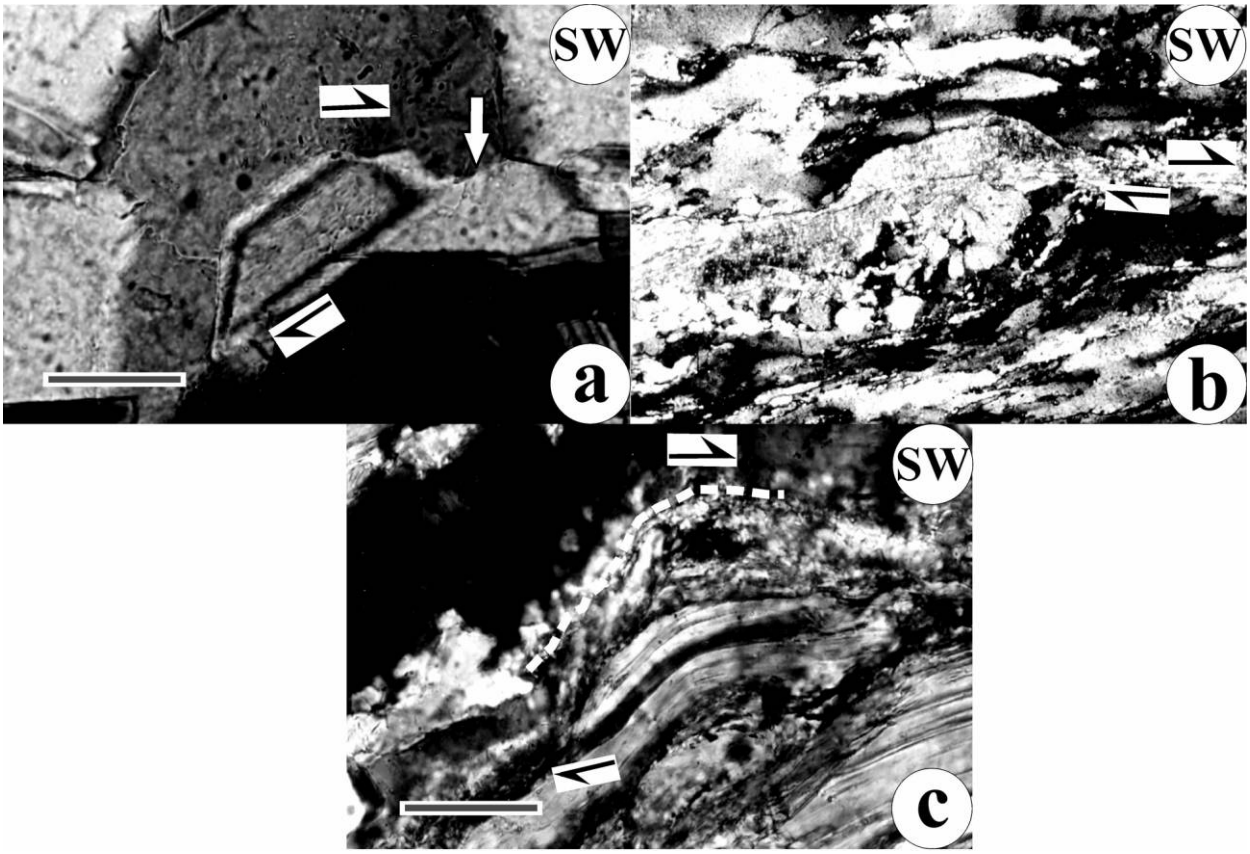

Figure 7. Top-to-southwest brittle shear sense displayed by trapezoidal micas whose longest margins dip northeast. Trace of *Y* planes extrapolated from outside the field of view; all photos in cross-polarized light. *a*, Margins of the muscovite trapezoid and the thrust plane given by that of a quartz grain (full arrow) are straight. Photo length = 1.3 mm; sample 10. *b*, Extensive recrystallization noted around the muscovite trapezoid but in an uneven way. Photo length = 2.5 mm; sample 9. *c*, The longest margin of the muscovite trapezoid is curved, and so are its cleavages. Profound recrystallization noted at the upper portion of the grain that has a sigmoid trace (white dotted line). Photo length = 1.3 mm; sample 7. A color version of this figure is available in the online edition or from the *Journal of Geology* office.

zoids of micas that lack contact with other underthrust mica grains and are found as isolated grains completely surrounded by quartzofeldspathic minerals (figs. 5*c*, 7*a*). The isolated mica trapezoids are speculated to have been translated relatively longer distances by thrusting so that the components of the once-continuous mica grain have been completely separated. Interestingly, mica fish devoid of any associated fish trails (= ductile shear planes) have also been reported isolated in quartzofeldspathic surroundings from mylonites (e.g., fig. 8*b* of Mukherjee 2011).

Except for the symmetric stacks (figs. 8, 9, 10*c*), the inclination (with respect to the *Y* planes) of the longest margins of these trapezoidal grains are reliable brittle shear sense indicators. All indicate a top-to-southwest sense (figs. 4–6, 7*c*, 8*b*, 10*a*, 10*b*) that matches with that documented from the HHSZ by Mukherjee (2007) and Mukherjee and Koyi (2010*a*). In addition, (i) cleavages, if visible within the trapezoids, (ii) some of the individual trapezoids in asymmetric stacks, and (iii) the supertrapezoids, taking into consideration the whole stack, all display the same shear sense (figs. 5*b*, 7*c*, 10*b*) and, therefore, are also reliable shear sense indicators.

A few trapezoidal grains display trails (or "tails") of fine-grained minerals emanating from their corners where their longest margins end (figs. 4*c*, 6*b*). As the trapezoids themselves are not products of ductile shear, their trails obviously cannot be related to ductile deformation. Instead, since these trails are aligned both along the *P* and *Y* planes, they can be considered as another reliable indicator of brittle shear sense. It is proposed that such trails have been fragmented from the corners of the trap-

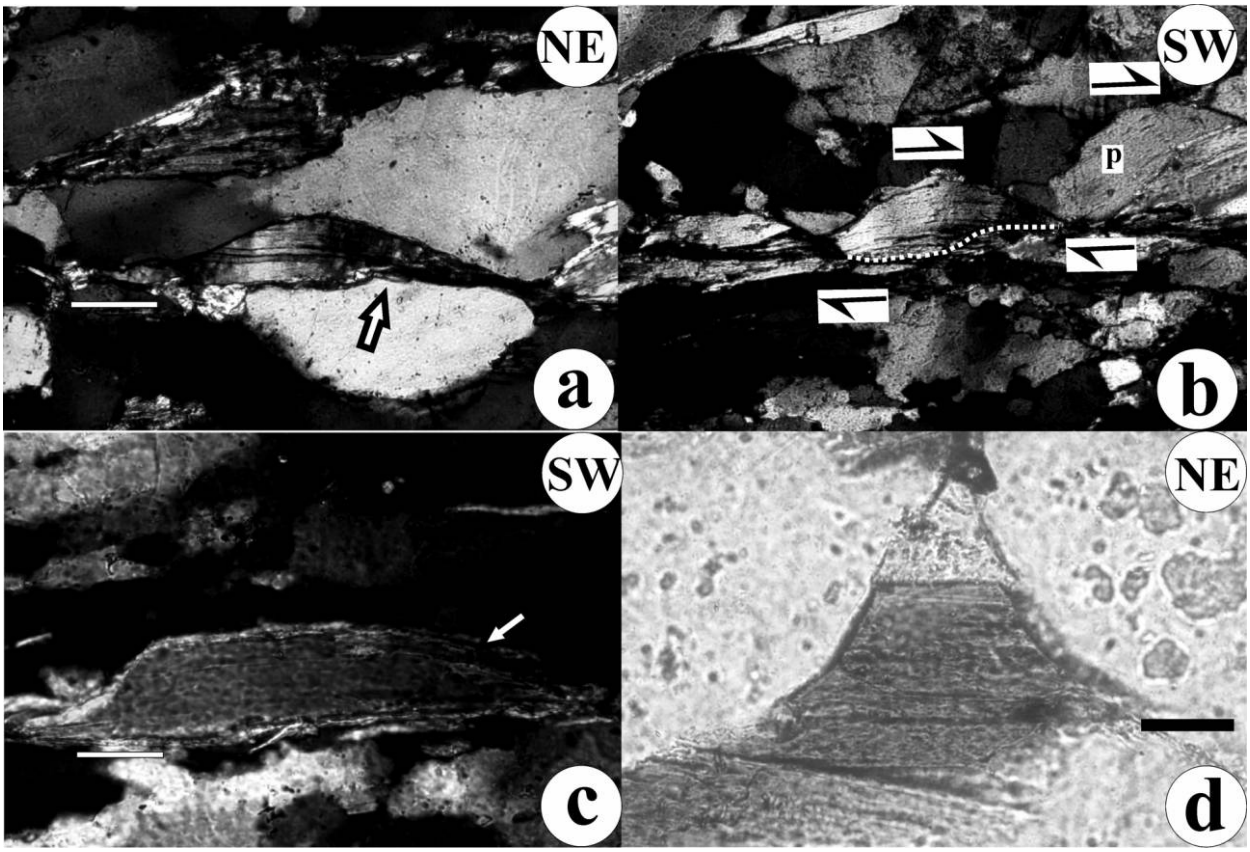

Figure 8. Trapezoid-shaped micas with their longest margins parallel to the northeast-dipping *Y* planes. *a*, Muscovite of nearly trapezoid shape sharply cuts across a quartz grain (arrow) along the *Y* plane. *b*, Weak asymmetry of the grain margin of the biotite trapezoid (dotted line) shows a top-to-southwest brittle shear sense that matches with that given by the adjacent single sigmoid quartz fish (grain p). *c*, A thin film of dynamic recrystallization mantles the muscovite grain; the mantled zone in the right-hand nonparallel margin of the trapezoid is thicker (full arrow) than the left-hand margin. *d*, Biotite trapezoid. In *a*, *c*, and *d*, the trapezoids are symmetric and themselves do not display any shear sense. In *a* and *b*, the cleavages of the mica grains are gently curved and are nearly parallel to the longest margins of the trapezoids. The *Y* plane (black line) in *d* is extrapolated from outside the field of view. *a*–*c* shown in cross-polarized light; *d* is in plane-polarized light. Photo lengths: *a*, 2.5 mm (sample 11); *b*, 5 mm (sample 13); *c*, 2.5 mm (sample 14); *d*, 2.5 mm (sample 15). A color version of this figure is available in the online edition or from the *Journal of Geology* office.

ezoids by brittle shear. Alignment of crushed minerals along the *P* and *Y* planes as trails might be a syntectonic process. Some mineral fish in mylonites are connected with stair-stepped trails (Lister and Snoke 1984; Mukherjee 2011) that define mylonitic foliations. The trapezoids, however, are normally not interconnected through trails (figs. 4–6, 7*a*, 8–10). Out of 312 trapezoids studied, only one had showed a notch at one of its corners (fig. 9*d*) that is convex toward the grain itself. Given that trapezoidal grains can possess trails without notches (figs. 4–8, 9*a*–9*c*, 10), notching cannot be an essential criterion to form trails.

Trapezoids may be thrust over a single mineral or an aggregate of minerals of the same species (figs. 4*d*, 6*a*–6*c*, 7*c*, 8*d*) or of different species (figs. 4*a*–4*c*, 5, 6*b*, 7*a*, 8*a*–8*c*). Underthrusting of more than one mineral against a single mineral grain (figs. 9*b*, 9*c*) would indicate possibly different intensities of frictional resistance along the longest margin of the latter overthrust grain during brittle shear. Where a trapezoidal mica is thrust over other minerals, it must cross-cut a third mineral grain. This must hinder the thrusting process. Therefore, brittle shear might not always be a smooth process at the grain scale.

The overriding grains may acquire smooth rounded contacts (especially figs. 7*c*, 8*a*, 8*b*) that may get stacked together (fig. 10*a*–10*c*). In a stack of trapezoids, the parallel margins of individual

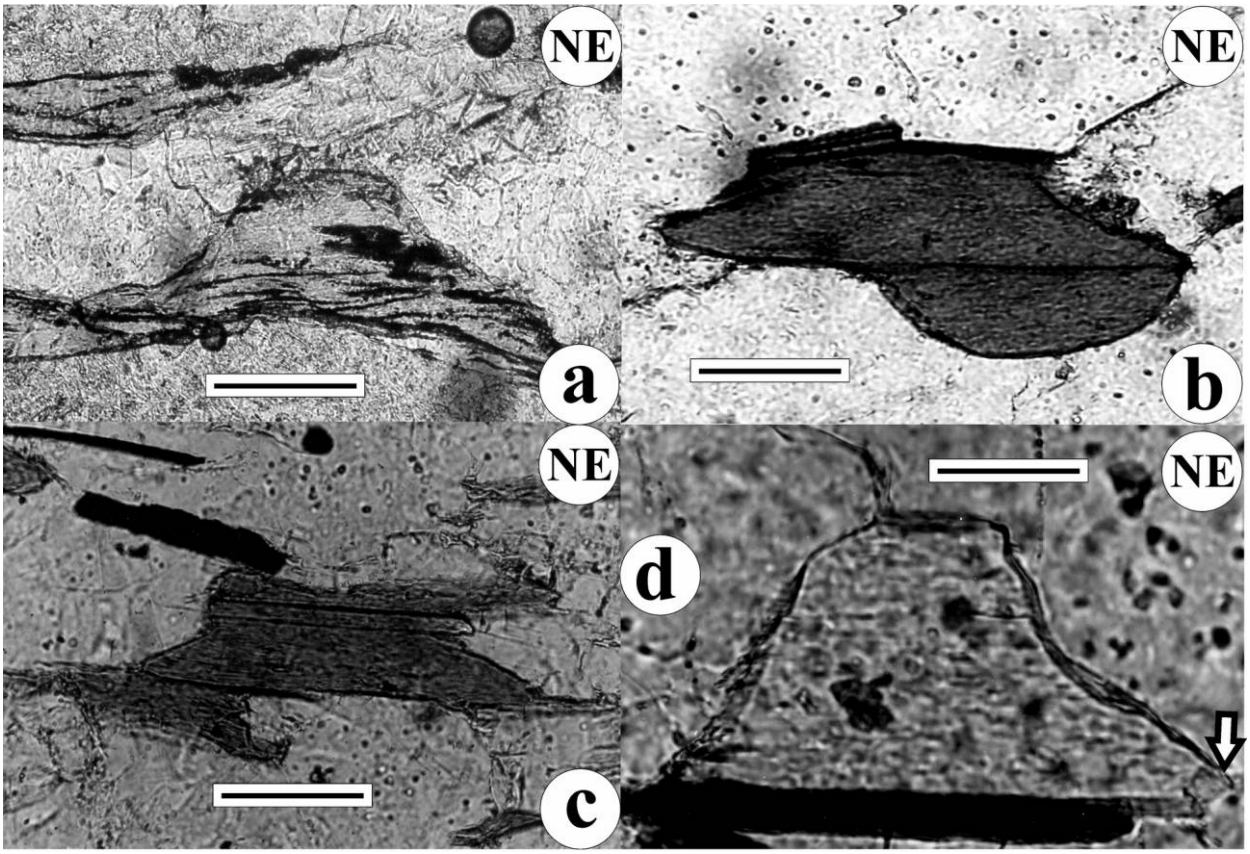

Figure 9. *a–c*, Trapezoid-shaped mineral grains with their longest margins parallel to the *Y* plane (white line, extrapolated from outside the field of view) do not reveal any shear sense, and no recrystallizations were noted around them. All photographs in plane-polarized light. *a*, Chlorite trapezoid; *b*, *c*, biotite trapezoids; *d*, muscovite trapezoid with a notch at its corner (full arrow). Interestingly, in *b*, the longest margins of two trapezoids are in contact. In *b–d*, the longest margins are partly in touch with another biotite grain and partly with a quartzofeldspathic mineral. On the other hand, in *d*, the longest margin is almost wholly in contact with another biotite grain. The nonparallel sides in all these trapezoids are curved to various degrees. Photo lengths: *a*, 2.5 mm (sample 18); *b*, 2.5 mm (sample 8); *c*, 2.5 mm (sample 15); and *d*, 1.3 mm (sample 7). A color version of this figure is available in the online edition or from the *Journal of Geology* office.

trapezoids are always in contact with each other. The exact geometry and orientation of individual trapezoids in the stack varies to some extent (figs. 5*b*, 10*a*–10*c*). In some grains, one of the margins is so small that the trapezoid looks triangular (fig. 6*d*). In such grains, the fourth margin is visible only at higher magnifications.

The cleavages of trapezoid grains always parallel the longest margin of the trapezoid (figs. 4–10). Since the longest margins act as the *P* planes and end up at angles to the *Y* planes, this suggests that brittle slip occurred along cleavage surfaces that also acted as *P* planes.

If the longest margins of the trapezoids are straight at a particular magnification, so are their cleavage planes (figs. 4, 5*a*, 5*b*, 6, 8*d*, 9*d*). Similarly, if the longest margins undulate or are kinked, so are the cleavage planes (figs. 6*b*, 7*c*, 8*a*, 8*b*, 9*a–9c*, 10*a*, 10*b*). The second set of these examples suggests that those trapezoid grains underwent internal crystal plastic deformation in sympathy with their brittle movement. Thus, mica trapezoids with curved or bent cleavages underwent ductile-brittle (or semibrittle) deformation rather than purely brittle.

Dynamic recrystallization developed thin mantles completely (figs. 7*c*, 8*c*, 10*d*) or partially (figs. 4*c*, 7*b*) around some of the individual trapezoidal micas. Dynamic recrystallization also affected a number of trapezoids in stacks (figs. 7*c*, 10*c*, 10*d*). Recrystallization was so extensive locally that the boundaries of individual minerals in those stacks become impossible to demarcate continuously. Recrystallized grains sometimes leave behind a pat-

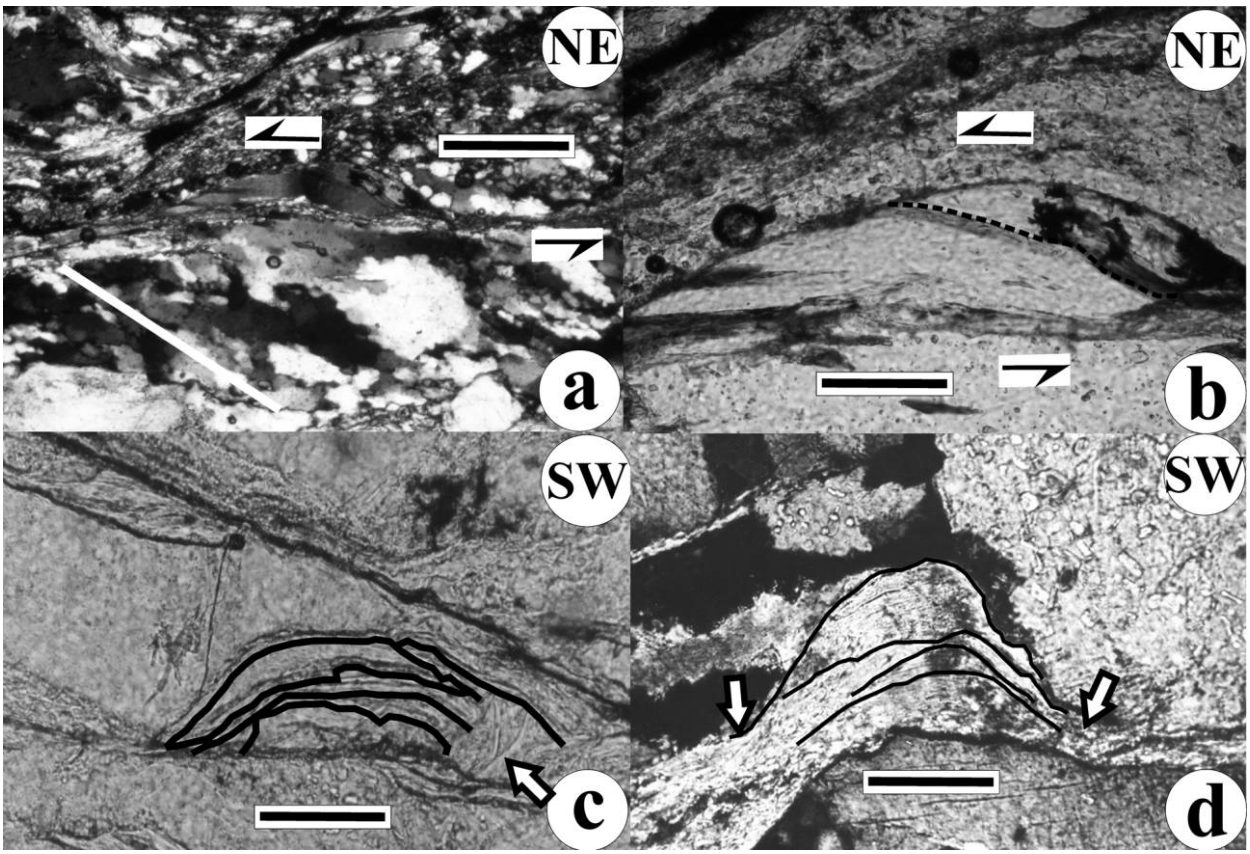

Figure 10. Subcircular (*a*, *b*, *d*) stacks and trapezoidal (*c*) muscovites with their longest margins nearly parallel to the *Y* plane (white line, extrapolated from outside the field of view). Top-to-southwest brittle shear displayed in *a*, *b*; *c* and *d* show indistinct margins of individual muscovite grains (full arrows). *a* and *d* photographed in cross-polarized light and *b* and *c* in plane-polarized light. Photo lengths: *a*, 5 mm (sample 4); *b*, 2.5 mm (sample 12); *c*, 2.5 mm (sample 8); *d*, 2.5 mm (sample 18). A color version of this figure is available in the online edition or from the *Journal of Geology* office.

tern indicative of the shear sense (fig. 7*c*). A mantle of irregular thickness (fig. 7*b*) suggests nonuniform strain hardening (Davis and Reynolds 1996).

The trapezoid-shaped minerals can be grouped on the basis of (i) their species, namely, biotite (figs. 4, 5*a*, 5*b*, 5*d*, 6, 8*a*, 8*b*, 8*d*, 9*b*, 9*c*), muscovite (figs. 5*c*, 7*a*–7*c*, 8*c*, 9*d*, 10*a*, 10*b*, 10*d*), or chlorite (fig. 9*a*) trapezoids; (ii) whether their long boundaries are in contact with another mineral of same species (figs. 4*d*, 6, 7*c*, 8*d*) or not (figs. 4*a*, 4*c*, 5, 6*b*, 7*a*, 7*b*, 8*a*–8*c*, 9*a*, 10); (iii) are their shapes perfectly trapezoidal (figs. 4, 5*a*–5*c*, 6*a*–6*c*, 7*a*–7*c*, 8*b*–8*d*, 9, 10*b*), or are they triangular (fig. 5*d*) or subcircular (fig. 8*a*); (iv) trapezoids with (figs. 5*d*, 6*b*) or without trails emanating from one or more corners (figs. 4, 5*a*–5*c*, 6, 7*a*–7*c*, 8, 9, 10); (v) trapezoid shape defined by either a single mineral (figs. 4, 5, 6, 7*a*–7*c*, 8, 9, 10*a*, 10*b*) or an aggregate (fig. 10*c*, 10*d*); and (vi) is the stack of minerals that define the trapezoid shape is symmetric (fig. 10*c*, 10*d*) and indicative of no shear sense, or asymmetric (figs. 4, 5, 6, 7*a*–7*c*, 8, 9, 10*a*, 10*b*) with a decipherable shear sense.

All these trapezoid-shaped micas come from the rocks of the HHSZ, which possibly underwent an initial phase of simple shear, and two subsequent phases of simple shear in conjunction with channel-flow extrusion. None of these trapezoid groups were found to be restricted to any particular tectonic subzones (MCT_U, $STDS_U$ and $STDS_L$ in fig. 3) inside the HHSZ. Thus, (i) biotite trapezoids were noted both from the basal part of the HHSZ, that is, near the MCT_U (fig. 5*a*; location 2 in fig. 3), as well as from its upper part near the location Akpa (fig. 4*d*; location 17 in fig. 3). (ii) A mica stack was identified (fig. 5*b*), nearly equidistant from the locations Karcham and Shongthong, which lies neither inside the $STDS_U$ nor the $STDS_L$ (location 6 in fig. 3). On the other hand, another mica stack, figure 10*d*, was found within the $STDS_U$ near Akpa (location 18 in fig. 3). (iii) Similar nonspecific oc-

currences of other microfabrics also exist in shear zones. For example, no correlation has so far been noticed between occurrences of the sigmoid-, lenticular-, and parallelogram-shaped mineral fish in any particular part of the ductile shear zones (Mukherjee 2011). Instead, genesis of different groups of trapezoids could be attributed to the microscopic inhomogeneity of the sheared rocks.

Figure 11 defines a number of parameters for trapezoidal minerals and aggregates. The "aspect ratio" is the ratio between the longest margin d to the perpendicular distance e between the parallel margins ($R_1 = de^{-1}$). While an R_1 value close to unity indicates that the trapezoid is nearly equant, values far from unity indicate that they are elongated.

To designate their angular parameters, the brittle shear Y planes near the trapezoids are to be oriented parallel to the east-west axis (either analyzer or polarizer) of the objective of the microscope, as in figure 11. The angle between the longest margin to the nonparallel margin dipping in the same direction as the longest margin itself is denoted "θ_1." The angle between the other nonparallel margin to the longest margin is denoted "θ_2." θ_1 and θ_2 are designated as internal angles. Obviously if the two internal angles approach equality, the nonparallel sides a and b tend to be the same. Following Mukherjee's (2011) in measurement of ductile sheared mineral fish, the "local orientation" (θ_3) of a trapezoid is designated as the angle between the longest margin (side d in fig. 11) to the Y plane. Where the shear plane is not visible, it can be extrapolated from some other part of the thin section (as done in figs. 4, 6, 7*a*–7*c*, 8*d*, 9*a*–9*c*, 10) to measure θ_3. The simple geometric relation amongst the internal angles and the length of the trapezoid margins is

$$d = c + (a\cos\theta_1 + b\cos\theta_2). \quad (1)$$

Measurements of aspect ratio and angles are straightforward for those trapezoids that escaped inward advance of adjacent quartzofeldspathic minerals and have nearly straight margins (figs. 4, 5*a*, 6*a*). However, there are examples of trapezoids where matrix minerals advanced most commonly along the nonparallel margins (figs. 5*c*, 8*d*, 9), and more rarely along the parallel margins (fig. 6*c*). The initial trapezoids in these cases can be estimated by reconstructing their straight margins by joining their furthest corners (see line q in inset of fig. 5*c*). The best fit straight line deciphered visually (line p in inset of fig. 5*c*) was not considered since it excludes a part of the mineral body.

Figure 12 presents a plot of aspect ratio (R_1; range: 0.5–21.4, mean: 5.4, mode: 4, median: 4.8) versus

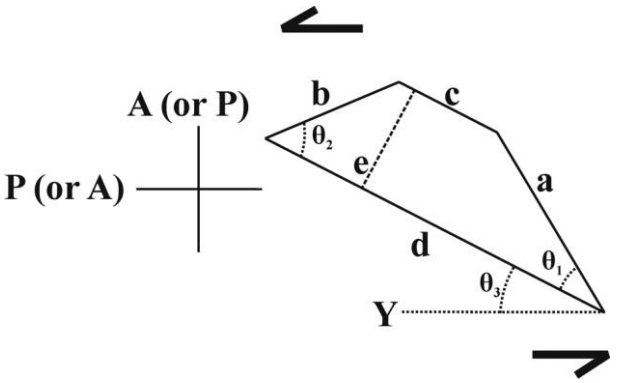

Figure 11. A trapezoid-shaped mineral grain is shown along with its different shape parameters. d and c are the lengths of the long and short margins that are parallel. The trapezoid is oriented in such a way that the Y plane (Y) is parallel to the east-west axis of the polarizer (P) or the analyzer (A). For this specific position of the trapezoid, a and b are its (lengths of) two nonparallel margins, d is the longest margin, and c is the fourth margin parallel to d. The angle between a and d is θ_1; between b and d the angle is θ_2; and local orientation θ_3 is between d and Y.

local orientation (θ_3; range: 0°–59°, mean: 16.8°, mode: 0°, median: 16°) of 317 mica trapezoids with well-defined margins. The figure shows the geometry of the trapezoids but has no genetic connotation. A similar approach with the different shape parameters that are unrelated genetically but are useful to delineate specific shapes in graphical forms have been well known in strain analyses (e.g., Flinn diagram in Hobbs et al. 1976), in representing other shear fabrics such as mineral fish (fig. 5 of Mukherjee 2011) and in sedimentology (e.g., Zing's diagram in fig. 3-18 in Pettijohn 1984). However, no such divisions are obvious in figure 12. Although a break in R_1 values are noted within about 16–19.5, only two plots exist for which $R_1 > 19.5$. Thus, the trapezoids are not grouped based on this break in R_1 values.

Future Work

A few unanswered questions about the trapezoidal grains are as follows. (i) What are their three-dimensional shapes? A study conducted by serial sectioning on individual trapezoid grains, like those on garnet porphyroblasts by Bell and Bruce (2006), should help answer this problem. (ii) Are these trapezoids a common feature in other brittle shear zones? Detailed thin-section studies of rocks from a number of brittle shear zones will be needed to determine whether trapezoidal minerals are common. (iii) How is the trapezoid geometry modified if the

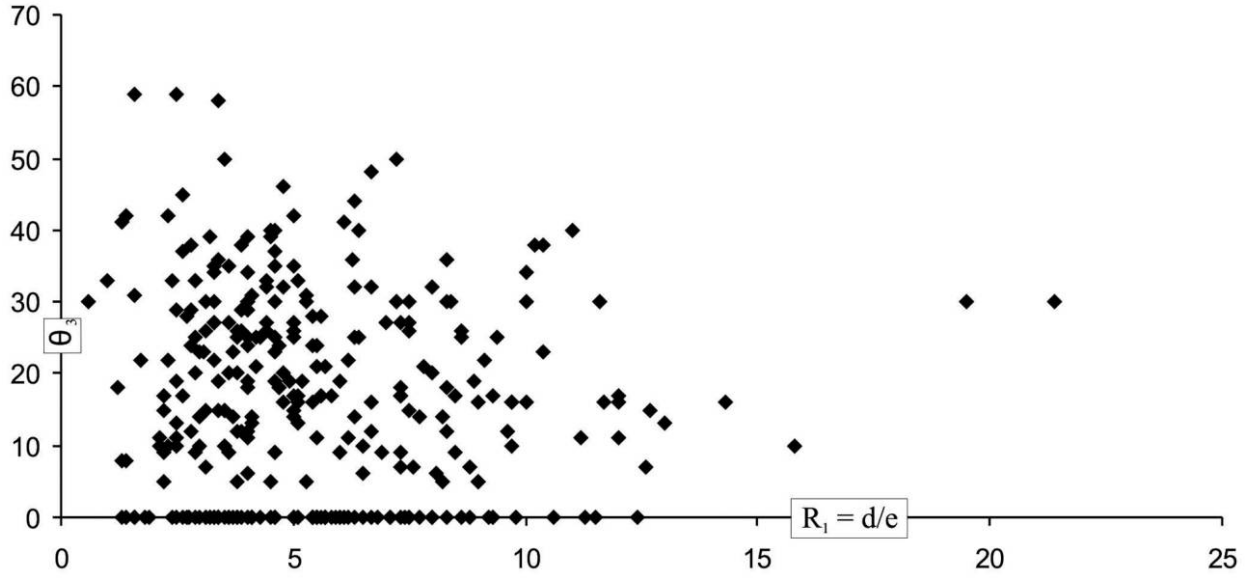

Figure 12. A plot of aspect ratio ($R_1 = de^{-1}$) versus local orientation (θ_3) for 317 trapezoidal micas.

brittle shear zone is subject to reactivation? (iv) Simulation of trapezoid geometry in geological models. The most crucial question is the exact kinematic process that gives rise to the thrust trapezoids. Particular attention is required on how the two nonparallel margins of these trapezoids are produced. Also, do the trapezoids keep increasing their aspect ratio ($R_1 = de^{-1}$) during prolonged brittle shear like ductile sheared mineral fish (Mukherjee 2011)? The software Elle (Bons et al. 2008) could be useful for understanding the progressive evolution of these structures and answer queries (iii) and (iv), as was shown for boudins by Koehn and Sachau (2008).

Conclusions

This work reports trapezoidal mineral grains, most often micas, from thin-sections of rocks in the Sutlej river section of the HHSZ, western Indian Himalaya. (1) Either (i) the longest margins of the trapezoids dip northeastward and show a top-to-southwest brittle shear, or (ii) the enveloping lines of these trapezoids coincides with the ductile shear *C* plane that later acted as brittle slip planes. These trapezoids are interpreted as microscopic thrust slices. The thrust grains may undergo intergrain slip, and cut across and shear over other grains. In a stack, the parallel margins of individual trapezoids remain in contact with each other. The longest margins, the cleavage planes, and the overall asymmetry of trapezoid (single grains or aggregates) act as the *P* planes and indicate brittle top-to-southwest shear. Any trails from the corners of the trapezoids are presumably clasts torn from the corners and define both the *P* and the *Y* planes.

(2) Some stacks of trapezoids are subcircular, and others have one of their margins so small that they appear triangles at low magnification.

(3) The cleavage planes of the trapezoidal minerals are normally straight but may be curved or kinked nonetheless parallel the longest margin of the trapezoid.

(4) Measurements on ca. 300 trapezoids of aspect ratio and a number of angles that partially characterize the trapezoid geometry exhibit wide ranges but do not relate to their genesis.

Further research is planned on the three-dimensional shapes of the trapezoids, how common they are in other shear zones, and most importantly, their likely initiation and evolution paths, preferably by computer simulations.

ACKNOWLEDGMENTS

This work was supported by a Indian Institute of Technology, Bombay, flexible seed grant: Spons/GS/SM-1/2009. P. Mukherjee assisted in handling data (fig. 12 but also a number of graphs not presented here). C. Talbot (retired from Uppsala University) made a positive and critical review that drastically improved the science and the presentation. Previous reviews by W. Xiao (Chinese Academy of Science), R. Greiling (Universität Karlsruhe), R. Norris (University of Otago), and four anonymous reviewers helped in shortening and strengthening the text.

REFERENCES CITED

Alonso, J. L.; Marcos, A.; and Suárez, A. 2006. Structure and organization of the Porma Mélange: progressive denudation of a submarine nappe toe by gravitational collapse. Am. J. Sci. 306:32–65.

Bahat, D. 1987. Jointing and fracture interactions in middle Eocene chalks near Beer Sheva, Israel. Tectonophysics 136:299–321.

Bell, T. H., and Bruce, M. D. 2006. The internal inclusion trail geometries preserved within a first phase of porphyroblast growth. J. Struct. Geol. 28:236–252.

Blenkinsop, T. G. 2000. Deformation microstructures and mechanisms in minerals and rocks. Dordrecht, Kluwer, 150 p.

Bons, P. D.; Koehn, D.; and Jessell, M. W., eds. 2008. Microdynamics simulation. Berlin, Springer, 405 p.

Chambers, J.; Parrish, R.; Argles, T.; Harris, N.; and Horstwood, M. 2011. A short duration pulse of ductile normal shear on the outer South Tibetan detachment in Bhutan: alternating channel flow and critical taper mechanics of the eastern Himalaya. Tectonics 30: TC2005.

Davis, G. H., and Reynolds, S. J. 1996. Structural geology of rocks and regions. New York, Wiley.

Fossen, H. 2010. Structural geology. Cambridge, Cambridge University Press. 274 p.

Godin, L.; Grujic, D.; Law, R. D.; and Searle, M. P. 2006. Channel flow, extrusion and extrusion in continental collision zones: an introduction. *In* Law, R. D., and Searle, M. P., eds. Channel flow, extrusion and extrusion in continental collision zones. Geol. Soc. Lond. Spec. Publ. 268:1–23.

Grasemann, B.; Fritz, H.; and Vannay, J.-C. 1999. Quantitative kinematic flow analysis from the main central thrust zone (NW-Himalaya, India): implications for a decelerating strain path and extrusion of orogenic wedges. J. Struct. Geol. 21:837–853.

Hippertt, J. F. M. 1993. "V" pull-apart microstructures: a new shear sense indicator. J. Struct. Geol. 15:1394–1403.

Hobbs, B. E.; Means, W. D.; and Williams, P. F. 1976. An outline of structural geology. New York, Wiley.

Hölgel, M.; Grasemann, B.; and Wagreich, M. 2006. Numerical modeling of clast rotation during soft sediment deformation: a case study in Miocene delta deposit. Int. J. Earth Sci. 95:921–928.

Holyoke, C. W., III, and Tullis, J. 2006. Formation and maintenance of shear zones. Geology 34:105–108.

Jessel, M. W. 1987. Grain boundary migration microstructures in naturally deformed quartzite. J. Struct. Geol. 9:1007–1014.

Koehn, D., and Sachau, T. 2008. Visco-elastic and brittle deformation. *In* Bons, P. D. ; Koehn, D.; and Jessell, M. W., eds. Microdynamics simulation. Berlin, Springer, p. 241–246.

Law, R.; Stahr, D.; Grasemann, B.; and Ahmad, T. 2011. Deformation temperatures and flow vortices near the base of the Greater Himalayan Crystalline Sequence, Sutlej Valley and Shimla Klippe, NW India (Vol. 13). Geophysical Research Abstracts. Munich, European Geosciences Union.

Lister, G. S., and Snoke, A. W. 1984. S-C mylonites. J. Struct. Geol. 6:617–638.

Mandal, N.; Chakraborty, C.; and Samanta, S. K. 2000. Boudinage in multilayer rocks under layer normal compression: a theoretical analysis. J. Struct. Geol. 22: 373–382.

McClay, K. R., ed. 1992. Thrust tectonics. London, Chapman & Hall.

Mukherjee, S. 2007. Geodynamics, deformation and mathematical analysis of metamorphic belts of the NW Himalaya. PhD thesis, Indian Institute of Technology, Roorkee.

———. 2008. Manifestation of brittle thrusting in microscale in terms of micro-duplexes of minerals in the higher Himalayan shear zone, Sutlej & Zanskar section, northwest Indian Himalaya. GeoMod2008: International Geological Modelling Conference (Florence, Italy, September 22–24). Boll. Geofis. Teor. Appl. 49:254–257.

———. 2010*a*. Microstructures of the Zanskar shear zone. J. Earth Sci. India 3:9–27.

———. 2010*b*. Structures at meso- and micro-scales in the Sutlej section of the Higher Himalayan Shear Zone in Himalaya. e-Terra 7:1–27.

———. 2011. Mineral fish: their morphological classification, usefulness as shear sense indicators and genesis. Int. J. Earth Sci. 100:1303–1314.

———. 2012*a*. Channel flow extrusion model to constrain dynamic voscosity and Prandtl number of the High Himalyan Shear Zone. Int. J. Earth Sci., forthcoming.

———. 2012*b*. A microduplex. Int. J. Earth Sci. 101:503.

Mukherjee, S., and Koyi, H. A. 2010*a*. Higher Himalayan Shear Zone, Sutlej section: structural geology and extrusion mechanism by various combinations of simple shear, pure shear and channel flow in shifting modes Int. J. Earth Sci. 99:1267–1303.

———. 2010*b*. Higher Himalayan Shear Zone, Zanskar Indian Himalaya: microstructural studies and extrusion mechanism by a combination of simple shear and channel flow. Int. J. Earth Sci. 99:1083–1110.

Passchier, C. W., and Trouw, R. A. J. 2005. Microtectonics. Berlin, Springer.

Pettijohn, F. J. 1984. Sedimentary rocks. New Delhi, CBS.

Powell, C. M. A. 1979. A morphological classification of rock cleavage. Tectonophysics 58:21–34.

Sengupta, S. 1983. Folding of boudinaged layers. J. Struct. Geol. 5:197–210.

Singh, K. 1999. Pull apart microstructures in feldspar from Chail Thrust Zone, Dhauladhar Range, Western Himachal Pradesh. *In* Jain, A. K., and Manickavasa-

gam, R. M., eds. Geodynamics of the NW Himalaya. Gondwana Res. Group Mem. 6:117–123.

Singh, S. 1993. Collision tectonics: metamorphic and geochronological constraints from parts of Himachal Pradesh, NW Himalaya. PhD thesis, University of Roorkee.

Srikantia, S. V., and Bhargava, O. N. 1998. Geology of Himachal Pradesh. Bangalore, Geological Society of India, 406 p.

ten Grotenhuis, S. M.; Trouw, R. A. J.; and Passchier, C. W. 2003. Evolution of mica fish in mylonitic rocks. Tectonophysics 372:1–21.

Trouw, R. A. J.; Passchier, C. W.; and Wiersma, D. J. 2010. Atlas of mylonites and related microstructures. Heidelberg, Springer, 297 p.

Twiss, R. J., and Moores, E. M. 2007. Structural geology (2nd ed.). New York, W. H. Freeman.

Vannay, J.-C., and Grasemann, B. 2001. Himalayan inverted metamorphism and syn-convergence extension as a consequence of a general shear extrusion. Geol. Mag. 138:253–276.

Vannay, J.-C.; Sharp, D. Z.; and Grasemann, B. 1999. Himalayan inverted metamorphism constrained by oxygen thermometry. Contrib. Mineral. Petrol. 137: 90–101.

Vernon, R. H. 2004. A practical guide to rock microstructure. Cambridge, Cambridge University Press.